Imaging and modification of polymers by scanning tunneling and atomic force microscopy

T. R. Albrecht, M. M. Dovek, C. A. Lang, P. Grütter, and C. F. Quate[a)]
Department of Applied Physics, Stanford University, Stanford, California 94305

S. W. J. Kuan and C. W. Frank
Department of Chemical Engineering, Stanford University, Stanford, California 94305

R. F. W. Pease
Department of Electrical Engineering, Stanford University, Stanford, California 94305

(Received 12 February 1988; accepted for publication 15 April 1988)

Direct imaging of ultrathin organic films on solid surfaces is important for a variety of reasons; in particular, the use of such films as ultrathin resists for nanometer scale fabrication and information recording requires that we understand their microstrucure. We have used the Langmuir–Blodgett technique to prepare monolayer and submonolayer films of poly(octadecylacrylate) (PODA) and poly(methylmethacrylate) (PMMA) on graphite substrates. Atomic scale images obtained with the scanning tunneling microscope (STM) and the atomic force microscope of the PODA films showed a variety of structures, including isolated narrow fibrils, parallel groups of fibrils, and an ordered structure consistent with the side chain crystallization expected with that material. The fibrils observed are interpreted as individual polymer chains or small bundles of parallel chains. Images of the PMMA samples show no ordered regions. By applying voltage pulses on the STM tip, we were able to locally modify and apparently cut through the PODA fibrils.

I. INTRODUCTION

Observation of organic adsorbates on conducting surfaces with the scanning tunneling microscope (STM) has been an intriguing area of research since the conception of the instrument. Previously, Langmuir–Blodgett (LB) bilayers of cadmium arachidate were imaged on a graphite substrate.[1] This work has recently been repeated and extended to phospholipid films as well as LB films with embedded proteins.[2] Sorbic acid,[3] copper phthalocyanine,[4] DNA,[5] di-methyl and di-ethyl phthalate,[6] and K-24 liquid crystals in their smectic phase[7] are examples of other organic materials for which STM images have been reported. Recently, an organic monolayer on an insulating substrate was imaged by atomic force microscopy (AFM).[8]

The LB technique for the formation of thin and uniform layers of amphiphilic molecules on solid substrates has come to prominence due to its potential applications in the field of microelectronics.[9] Generally, the LB films formed by amphiphilic monomers have poor thermal and mechanical stability, which is a major drawback for practical applications. To form stable and robust films two ideas have been proposed. One is to use molecules which are polymerized by irradiation with ultraviolet light or an electron beam after transfer to a solid substrate.[10] The other technique, which was used in these experiments, is to transfer the preformed amphiphilic polymer to substrates by the LB technique.[11]

In this paper, we report the first STM and AFM images of polymers deposited with the LB technique on a graphite substrate. The polymer studied was poly(octadecylacrylate) (PODA). With our STM we have also imaged LB deposited atactic poly(methylmethacrylate) (PMMA), which is a commonly used electron-beam resist,[12] but have found only disordered structures. We therefore decided to focus our studies on the polymer PODA whose strong alkyl side chain interactions are known to yield an ordered structure in the bulk.[13]

PODA structures on graphite were imaged by both STM and AFM, confirming the reproducibility of the data by two different microscopy techniques. Several structures were observed on samples prepared by three polymer deposition techniques.

It was possible to perform molecular manipulation of isolated polymer fibrils on graphite in the STM. Application of a voltage pulse on the STM tip resulted in modification of the polymer at the location of the pulse. Similar surface modifications with the STM, including molecular attachment of di-methyl and di-ethyl phthalate to the graphite substrate,[6] deposition of metallic features from the gas phase,[14] "lithography" on gold and graphite substrates, and electrochemical gold deposition on a gold substrate,[15] have been previously reported.

II. SAMPLE PREPARATION

The LB films were atactic PODA (Ref. 16) with a weight average molecular weight (M_w) of 23 300 and a number average molecular weight (M_n) of 13 000, and were deposited using a Langmuir trough.[17] The monomer repeat unit [see Fig. 1(a)] has a molecular mass of 324, which corresponds to about 40 repeat units and a 120-Å total chain length for the polymer.

The PODA was spread on the purified water (pH 6.4) surface from a dilute (0.5 mg/ml) solution in chloroform. Several slow (30 cm^2/min) compression and expansion cycles were repeated until the pressure-area isotherm was re-

[a)] Also at Department of Electrical Engineering, Stanford University and XEROX Corp., Palo Alto Research Center, Palo Alto, CA 94304.

 0021-8979/88/151178-07$02.40

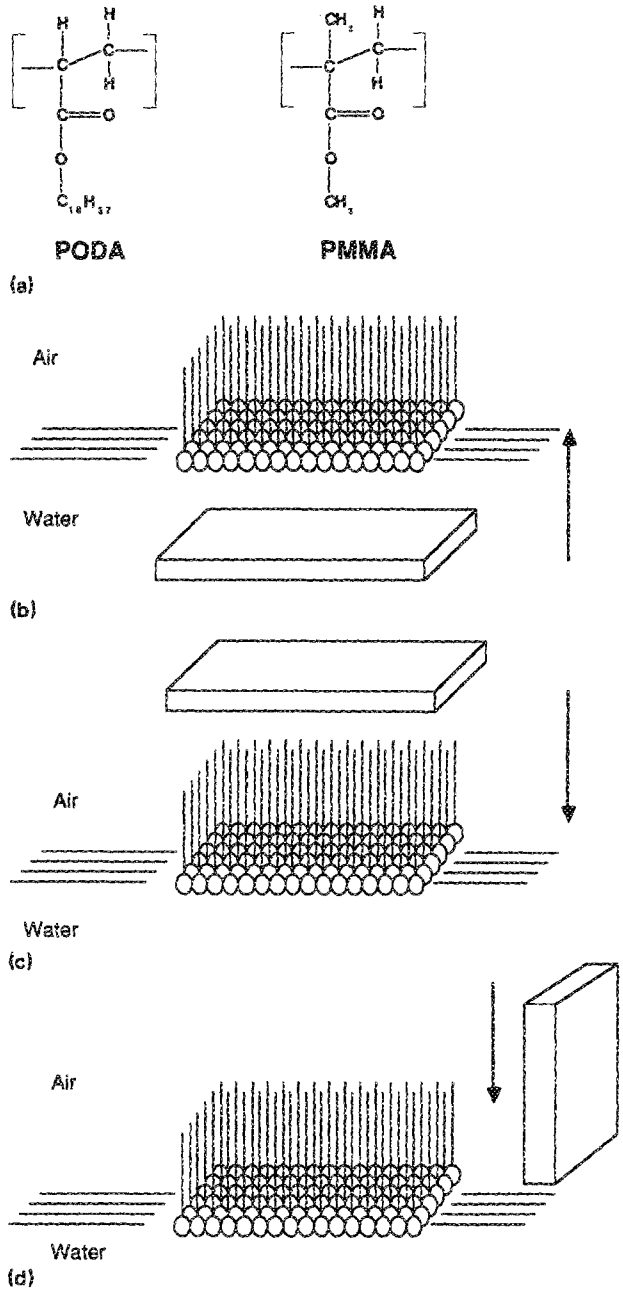

FIG. 1. (a) Molecular structure of the monomer repeat unit of PODA and PMMA. Samples were prepared by (b) horizontal lifting from the water subphase, (c) horizontal dipping from the top, or (d) vertical dipping.

producible. During film transfer the pressure was held constant at 20 dyn/cm.

We used highly oriented pyrolytic graphite (HOPG) as the substrate. It was freshly cleaved with tape rendering surfaces atomically flat over thousands of angstroms.[18] Three different types of films were prepared and studied. The first type of film [see Fig. 1(b)] was prepared by raising a horizontally held graphite substrate from the bottom of the LB trough. Due to the hydrophobic character of the surface, the water slips off the graphite leaving a submonolayer polymer film on the surface. The second type of film [see Fig. 1(c)] was prepared by lowering the horizontally held graphite to bring it into contact with the spread film and raising it again. The third type of film [see Fig. 1(d)] was transferred by first dipping the graphite vertically into the water subphase and then lifting it vertically out. The latter two methods are expected to yield mono- and bilayer coverages since the hydrophobic side chains establish direct contact with the graphite. The dipping speed for all three methods was 1 mm/min.

Attenuated total reflection (ATR) infrared spectroscopy performed on these samples showed strong symmetric and antisymmetric CH_2 stretching modes and weak C = O vibrational peaks, which were not observed on clean graphite.

III. FILM STRUCTURE

The identification and characterization of flexible polymers on surfaces is inherently complicated because of uncertainties in (1) characterization of the intrinsic chain configuration for high polymers having many repeat units, (2) determination of the mode of organization of polymer chains in the Langmuir film prior to transfer, and (3) understanding the individual and cooperative chain rearrangements which occur during transfer of the film to the substrate.

In polymers with very long side chains it has been well established that dispersive interaction between the side chains can lead to crystallization of the bulk material. Such interaction, referred to as side chain crystallization, has been reported for PODA.[13] The extent of crystallinity has been estimated to be 38% based on specific volume measurements.[19]

There is general agreement that the side chains are perpendicular to the chain backbone.[13,20] Since the PODA sample is atactic it is unlikely that the backbone participates in the crystalline packing. In fact, Hsieh, Post, and Morawetz[20] have proposed that the backbone as well as the first nine methylene groups are disordered. The crystalline regions are formed from the outer portions of side chains of the same as well as different polymer chains and are packed in a hexagonal array. The minimum size of such a bundle would be about 11 Å diam.

For the pseudo-two-dimensional Langmuir film, there is some degree of simplification, but significant structural issues remain unresolved. Mumby, Swalen, and Rabolt[21] found that mono- and multilayer PODA Langmuir films formed by spreading from a dichloromethane solution could be transferred to both hydrophilic and hydrophobic surfaces. They used grazing incidence reflection infrared spectroscopy to show that for LB PODA films on a hydrophilic aluminum substrate, the carbonyl bonds are oriented perpendicular to the surface, as are the hydrocarbon tails. Since their results for multilayer structures were similar to those for a monolayer, they concluded that there was no mismatch between layers; i.e., the monolayer structure was replicated throughout the assembly. Since the hydrocarbon chains are oriented perpendicular to the substrate, it seems likely that they interact in a manner similar to that which induces side chain crystallization in the bulk. However, a significant difference is that the side chains protrude from the backbone in two opposing directions in the bulk, whereas on the water surface they are expected to be relatively parallel. This has

important consequences for interpretation of the structures formed upon transfer from the water to the graphite. The infrared spectroscopy was unable to provide much information about the backbone structure. However, pressure-area isotherms indicated no significant contribution from backbone overlap. One could conceive of a variety of relatively ordered backbone organizations that would allow close packing of the side chains with no backbone crossovers, particularly since PODA backbones are relatively short. No direct evidence for this exists, however.

IV. STM AND AFM INSTRUMENTATION

We used a pocket size STM with single-tube scanner operated in air, which routinely renders atomic resolution on graphite.[22,23] Due to the rough topography of the surfaces studied and the large scale scans used, we were unable to operate in the normal fast scan mode. The horizontal line scan and the frame rate were lowered to 200 and 1 Hz, respectively. The feedback bandwidth was set to approximately twice the horizontal scan rate. The contrast information was extracted from the current error signal as it is typically done in constant height mode. Images were taken with a bias of approximately 0.3 V and tunneling currents between 0.25 and 0.5 nA. Images taken at higher currents were unstable.

Our AFM, which is similar in construction to the STM used in these experiments, has been previously used to image several crystalline surfaces, including graphite, with atomic resolution.[24] The AFM was operated in air using the fast scan variable deflection repulsive contact mode. In this mode, images of the sample are obtained by measuring angstrom scale changes in the deflection of a cantilever beam as the tip of the lever is held in contact with the sample by applying a small force. The deflection of the lever changes in response to surface topography and is detected by tunneling to the backside of the cantilever. The cantilevers used in these experiments were microfabricated "V-shaped" SiO_2 levers described previously.[8,24,25] Atomic resolution images were obtained using forces in the range of 2×10^{-8}–1×10^{-6} N, with best results near the upper end of this range. Horizontal and vertical scanning frequencies were 1800 and 18 Hz, respectively. A feedback system with slow response was used. The contrast information was extracted from variations in the tunneling current.

In both instruments, images were displayed using a video image processor with a temporal filter,[26] which continuously converts the data into a real time video grayscale image. The video images are recorded on videotape and can later be transferred to a graphics workstation for further image processing and subsequent photography.

V. STM STUDIES OF POLYMER FIBRILS ON GRAPHITE

With the STM, we observed submonolayer coverages of PODA on the surface of the horizontally dipped samples described in Sec. II. Three of these samples were prepared by horizontal raising and one was prepared by horizontal lowering. On samples prepared by the first technique, we observed several areas of bare graphite. Also observed were several areas exhibiting isolated fibrils that ranged in length from one hundred to several hundred angstroms with the graphite background clearly visible on either side. In other regions the fibrils had formed small bundles which were in turn parallel to other bundles in the vicinity. Occasionally, the orientation of the chains with respect to the substrate remained constant over distances of several thousand angstroms. Rotating the scan direction did not affect the direction of the bundles, ruling out the possibility that the scanning influenced the orientation of the chains or caused some similar imaging artifact.

Figure 2(a), shows a portion of an isolated narrow fibril and the graphite lattice background which was used to determine the geometric calibration. The fibril width is 8 ± 2 Å and although it is tempting to conclude that it is an image of a single polymer chain, it is also possible that the fibril represents a small bundle of a few chains. The shadow that is observed to the right of the chain is caused by the delayed response of the feedback to the strong current signal from the fibril. This response also causes the apparent distortion of the graphite lattice to the right of the fibril. No exact height information can be extracted from the signal because of the mixed imaging mode used and the elastic deformation of soft layered surfaces, such as graphite, imaged by STM in air.[27] Moreover, the derivation of height information depends on the nature of the tunneling barrier, which is not well understood. Figure 2(b) shows a parallel array of fibrils. If part of an array is viewed at higher magnification,

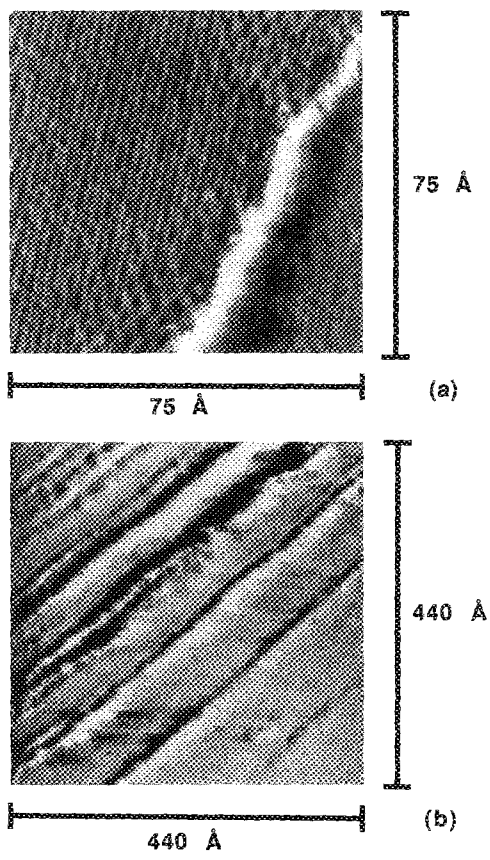

FIG. 2. STM images of PODA submonolayers on graphite: (a) An isolated fibril on the otherwise clean graphite. (b) In other areas, the much more common larger fibrils are seen, which are interpreted as bundles of chains.

images similar to Fig. 2(a) are obtained where the graphite background is clearly resolved and very closely spaced narrow fibrils are visible. While scanning regions containing isolated fibrils, we obtained images which were probably produced by multiple tips.[28,29] In these images the intensity of the chain was reduced with respect to the background and one could see the graphite lattice superimposed on the chains themselves. Such artifacts can result from simultaneous imaging by two or more tips, one of which scans over the adsorbate while the others scan over clean graphite.

It seems clear that the structures observed in Fig. 2 are due to the PODA chains that have been deposited on the graphite. A detailed picture of the polymer side chain structure is more difficult to present, however. During the horizontal lifting of the graphite substrates, one expects that the flow of the water would cause breakup of the organized PODA film. Although this flow could induce ordering in the orientation of the chains, one would expect that the side chain interactions between groups of different backbones that existed in the Langmuir film on the water surface would be preserved. Thus, the smallest feature could correspond to several chains with parallel backbones that are not necessarily in lateral registry. The narrow width is consistent with the expectation that the side chains do not extend horizontally from the polymer backbone, but are oriented away from the substrate. Side chain interaction could then produce the minimum size hexagonal bundle that has been suggested as the important structural feature in the bulk. The larger bundles would then result from aggregation of these small features, again as a result of side chain interaction.

Another interpretation is that the smallest feature is a single chain. One would expect that in the absence of the stabilizing side group interactions found for multiple chain aggregates, the hydrophobic side chains would lie horizontally on the graphite surface. Since hydrocarbons and water, normally present on samples in air, are usually not imaged in STM, it is conceivable that only the PODA backbone appears in the image. In the absence of accurate height information and understanding of the exact charge transport mechanism, one cannot unequivocally discriminate between the single chain and the multiple chain models.

One of the samples prepared by horizontal raising in the LB trough exhibited an isolated highly ordered region of approximately 300 Å × 300 Å, shown in Fig. 3(a). The spacing between rows (measured along a line joining the upper right-hand and lower left-hand corners) is one to two times the side chain length. This spacing is in agreement with a two-dimensional version of a model proposed for the crystalline bulk.[13] The details of the polymer organization in this ordered region are difficult to determine. It is not clear, for example, whether any of the linear features seen in the array are polymer backbones or whether they are groups of side chain crystallites.

The sample that was prepared by lowering into the LB trough, on the other hand, displayed a number of different structures, including areas of clean graphite, isolated fibrils, densely packed disordered regions, and several ordered structures different from that shown in Fig. 3(a). Figure 3(b) shows a diamondlike structure which might be interpreted as a nucleation seed of larger scale structures which are known to exist in bulk polymer single crystals.[30]

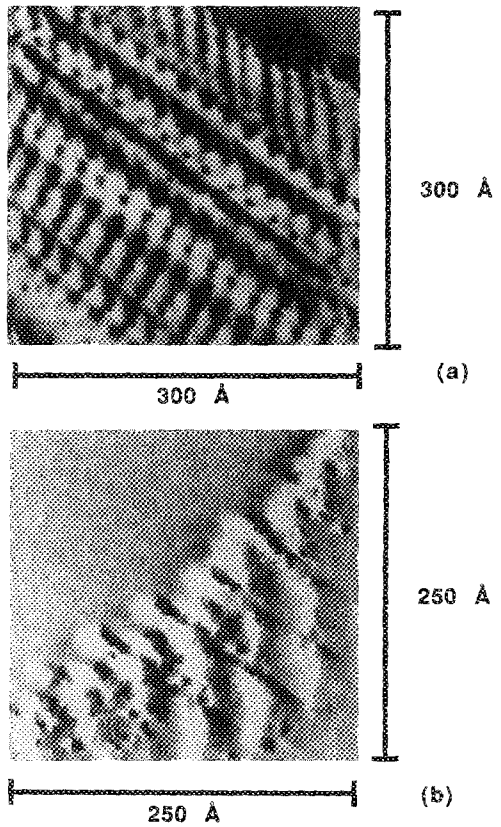

FIG. 3. STM images of two ordered regions obtained on samples with submonolayer coverage: (a) a two-dimensional ordered overlayer suggestive of bulk ordering, (b) possible diamond-shaped nucleation seed of larger scale bulk structures.

The observation of these ordered structures suggests that the transferred film has properties characteristic of the bulk over small parts of the surface.

The vertically dipped samples exhibited full coverage. No clean graphite regions were observed on these samples except at the edges where the transfer might not have taken place successfully. STM images of vertically dipped samples were somewhat less noisy than the submonolayer samples prepared by horizontal dipping. This noise reduction, which is attributed to the greater stability and smooth topography of the full coverage films, allowed us to observe more of the fine scale features of the adsorbates themselves. Particularly prominent on these samples were regions containing highly parallel features.

Figure 4(a) shows a boundary region between two regions exhibiting different morphologies. Both regions appear to contain overlapping plates (or wide fibrils); however, the packing appears denser in the upper domain. The lower domain shows the same parallel ordering which was observed to some extent on all samples. Some fine scale structure is visible within individual plates. One may speculate that the more densely packed array visible in the upper domain is the result of greater overlapping caused by buckling during compression or transfer of the film to the substrate. The plates in both domains may be quite similar, with

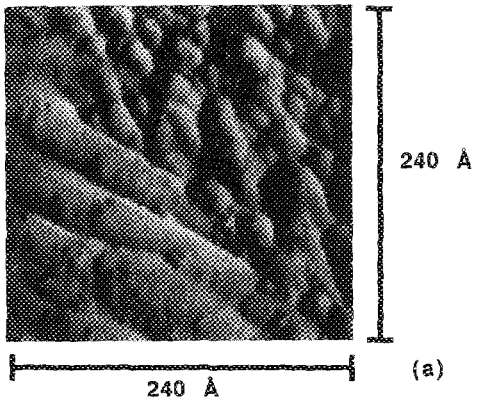

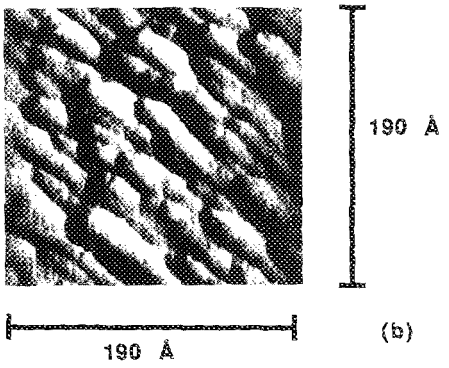

FIG. 4. STM images of PODA bilayers on graphite: (a) a sharp domain boundary separates two regions with differing morphology, (b) shows a densely packed, but not highly ordered, array of overlapping structures.

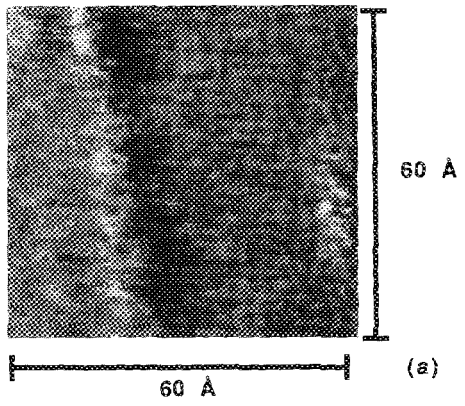

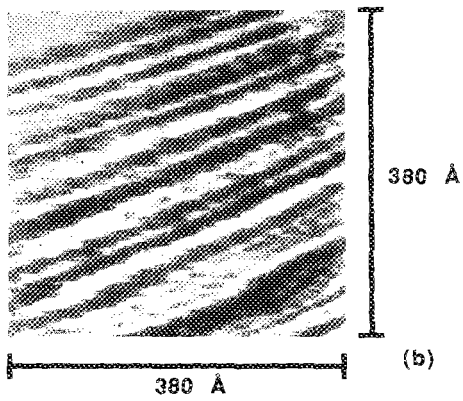

FIG. 5. AFM images of submonolayer PODA on graphite: (a) an isolated fibril stretched across the surface, (b) parallel fibrils on the surface.

variations in overlapping differentiating the two domains. Figure 4(b) shows another region elsewhere on the sample similar to the upper domain of Fig. 4(a), but with a slightly different packing.

VI. AFM STUDIES OF POLYMER FIBRILS ON GRAPHITE

For the AFM studies, another sample with submonolayer coverage of PODA was prepared by the horizontal raising technique. This sample was imaged by AFM for the purpose of comparing the observed structures with those seen by STM and to demonstrate the usefulness of AFM for imaging adsorbed polymers. On approximately 50% of the surface, clean graphite was observed. AFM images of clean graphite showed no geometric distortion and were comparable in signal-to-noise ratio with good quality STM images of graphite. A variety of structures was observed in other regions of the sample. Figure 5(a) shows a single fibril 5–10 Å wide stretched across the graphite surface. The similarity of this image to Fig. 2(a) demonstrates the reproducibility of the observed structure and the good correlation between AFM and STM images of samples prepared in this way. Although it is not possible to determine with certainty from the image that the fibril is a PODA polymer or bundle of polymers, similar structures are seldom encountered on clean graphite except in the rare case of a grain boundary,[31] which can be identified from its characteristic change of crystal orientation. Such fibrils were observed singly and, more frequently, in parallel arrays as shown in Fig. 5(b), which is similar to the STM images of parallel arrays on samples with submonolayer coverage [e.g., Fig. 2(b)]. The spacing of these large (length > 100 Å) fibrils in arrays was 10–30 Å. Smaller fibrils were observed in small parallel arrays with spacings of 3.5–5 Å. Figure 6(a) shows a region where several isolated fibrils having different orientations appear to overlap one another.

AFM images of surfaces that are not atomically flat are difficult to interpret because of two effects: (1) simultaneous imaging from multiple contact points between the tip of the cantilever and sample, and (2) imaging of apparent superlattices around disruptions in the graphite lattice. The first of these effects is more pronounced in the AFM than the STM because of the nonideal geometry of the tip of the cantilever used in these experiments. This tip is much less sharp macroscopically than a conventional STM tip, since forming a sharp tip on the cantilever presents difficult fabrication problems.[32] In the worst case, the cantilever and sample can be considered as two rough surfaces in contact with one another, and the image is a convolution of the topography of both surfaces. While images of atomically flat graphite are only subtly affected by multiple tips,[29] images of rougher surfaces can be completely altered. For example, the apparently overlapping chains in Fig. 6(a) may result from simultaneous imaging of nonoverlapping chains in two separate regions of the sample by two protrusions on the tip of the cantilever. Stronger evidence for this effect is shown in Fig. 6(b). The three structures visible could be three identically bent fibrils adsorbed on graphite with exactly the same ori-

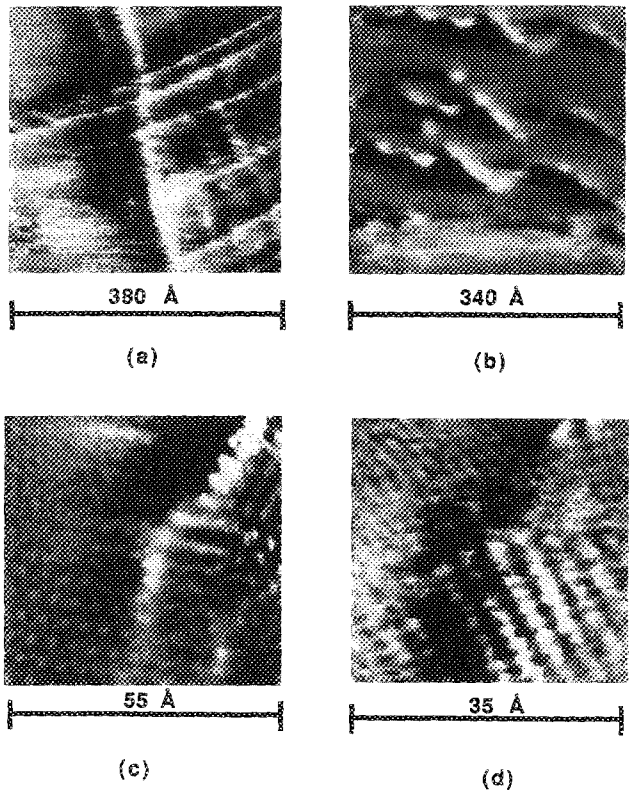

FIG. 6. Examples of AFM images which are difficult to interpret: Isolated chains (a) may actually overlap or result from a superposition of nonoverlapping chains due to multiple tips. A triple image (b) of a single feature is likely caused by three tips. In (c), the brighter dots visible in the lower left (in contrast to the normal graphite seen in the upper left) form an apparent $\sqrt{3}$ superlattice attributed to scattering of electron states in the graphite. The array of dots in the lower part of (d) may be a distorted superlattice or the actual small scale structure of adsorbates.

entation, but it is more likely that a single adsorbate was imaged by three asperities on the cantilever tip. The probability for multiple tip imaging can be reduced either by improving the tip geometry or by using substrates which undergo less elastic deformation due to the forces involved in the AFM. Such deformations, which are thought to occur on the surface of layered materials such as graphite,[27] increase the contact area between tip and sample.

The appearance of superlattices near lattice defects is known to occur in STM images of graphite.[33] In these experiments, however, the effect was observed more often in AFM images than STM images of PODA on graphite. The adsorbate visible in the upper right-hand corner of Fig. 6(c) is believed to be responsible for the apparent $\sqrt{3}$ superlattice visible in other areas of the image due to scattering of the electron states in the graphite at the adsorption sites.[33] Other structures can be difficult to distinguish from these superlattices, such as the array of bright spots seen in Fig. 6(d). These spots exhibit a 4 Å × 2 Å periodicity. One may speculate that the array of spots shows the structure of chains lying flat on the graphite, which seems unlikely in light of previous studies, or are due to individual side chains oriented perpendicular to the substrate. In the latter interpretation, deformation of the graphite surface allows the AFM to image both the graphite substrate and the side chains structures, which are expected to extend ~20 Å vertically. However, one cannot rule out the possibility that the spots are caused by an apparent superlattice whose geometry is distorted by friction or other effects in that region.

VII. MODIFICATION OF POLYMER FIBRILS WITH THE STM

The samples that were used for this experiment were prepared by the horizontal raising technique. A rectangular voltage pulse of 100-ns duration was applied to the STM tip while it was over part of an isolated chain bundle. Although the graphite background was visible in various one-dimensional amplitude traces, it was not visible in the two-dimensional images due to the lack of continuous high resolution over the averaging period of our display device. The low signal-to-noise ratio was due to tip instabilities caused by voltage transients during pulsing.

Figure 7(a) is a 400 Å × 400 Å image showing a bundle of fibrils before a pulse is applied to the tip. Figure 7(b) shows the same area after the pulse is applied. In the second image it appears that the bundle width has approximately halved, which may be an imaging artifact caused by a change in tip geometry during the pulse (e.g., removal of a second tip). The pulse disrupts the highly parallel structure over a 50-Å radius region, and appears to have broken the fibril at the place where the pulse was applied. The effect may be similar to what occurs when PMMA is bombarded with electrons in an *e*-beam exposure system.[34] During *e*-beam

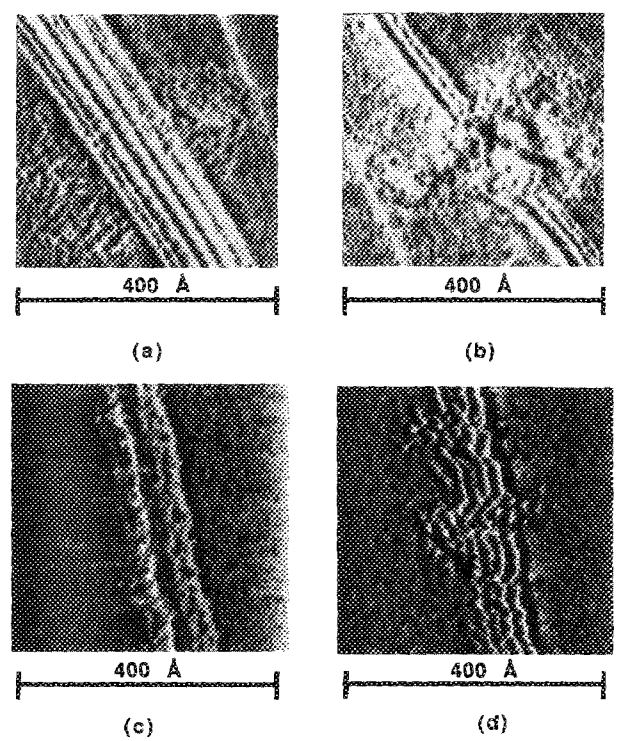

FIG. 7. Modification of polymers with the STM: A wide fibril (a), which is interpreted as a bundle of chains, is visible before a pulse is applied to the tip. In the same area after the pulse (b), the fibril has been disrupted, and perhaps cut through, at the location where the pulse was applied. At a different location (c) along the same fibril, additional disruptions (d) are visible after two more pulses are applied at different points.

exposure, single bonds in the polymer chain are broken, and monomers and larger building blocks are released. Figures 7(c) and 7(d) show the same effect in a region further along the chain. Two pulses were applied to the tip between those two images. The cause of the debris appearing around the rupture is not immediately obvious, but may be related to the negative action of the resist.

The voltage threshold for this effect was measured to be 4.1 ± 0.2 V. The peak value of the tunneling current during the pulse was approximately 200 nA. Assuming the pulse energy is distributed over a 50-Å radius region, and using a monolayer film thickness (20 Å), the energy density for a single pulse is calculated to be 6×10^5 J/cm^3. This energy density, although very high for conventional exposure of PMMA, is consistent with the density recently used in a larger scale lithography experiment with an STM on 200-Å-thick PMMA films.[35] In the case referred to, 10 pA of current, a constant 20-V tip bias, and a scan speed of 1 μm/s were used for exposure. Following the chemical development of the resist, 200-Å lines were observed by scanning electron microscopy (SEM).

The tip voltage pulsing technique is repeatable and can be used to deliberately cut the fibrils at a number of different locations. The ability of the STM to cut individual narrow fibrils of PODA on graphite suggests a new way in which the STM may be used for lithography on a molecular scale. Using well-characterized film deposition techniques we envision the possibility of lithographic patterning with a resolution of 100 Å or better.

VIII. CONCLUSIONS

LB deposited PODA on graphite has been imaged using two new powerful tools: STM and AFM. The results suggest that these two instruments can be used to observe the orientation and morphology of organic chains. We have used three different deposition techniques, each of which is expected to give a different surface coverage. The STM and AFM images are consistent with what we know about side chain interaction of PODA in bulk form and in Langmuir–Blodgett films. Submonolayer coverages result in parallel isolated and bundled fibrils with a visible substrate background and occasional ordered regions, while mono- and bilayer coverages result in overlapping structures. Similar structures have also been observed on epitaxial Au (111) on mica and MoS_2. These results and film structure formation mechanisms will be discussed in a subsequent publication.[36] The results also point out poorly understood features of the instruments, such as multiple tip imaging, especially in the AFM. Furthermore, we have demonstrated a mechanism for manipulating the polymers with the STM which seems to be of a similar nature as *e*-beam lithography on acrylates.

ACKNOWLEDGMENTS

The authors would like to thank D. P. E. Smith and A. Bryant of the Tunneling Microscope Company for donating the STM, A. W. Moore for providing the HOPG, L. La-Comb for his help with the image processing, H. Chen for his help with the FTIR, P. Maccagno for instruction in the LB technique, and T. W. Hänsch and J. Foster for useful discussions. We acknowledge the support of a National Science Foundation Graduate Fellowship (TRA), an IBM Predoctoral Manufacturing Fellowship (MMD), and a German National Scholarship Foundation overseas fellowship (CAL). This project was supported by the Defense Advanced Research Projects Agency, the NSF-MRL Program through the Center for Materials Research at Stanford University and the National Science Foundation ECS 86-08318.

[1] D. P. E. Smith, A. Bryant, C. F. Quate, J. P. Rabe, Ch. Gerber, and J. D. Swalen, Proc. Natl. Acad. Sci. **84**, 969 (1987).
[2] J. K. H. Hörber, C. A. Lang, T. W. Hansch, W. M. Heckl, and H. Möhwald, Chem. Phys. Lett. **145**, 151 (1988)
[3] D. P. E. Smith, M. D. Kirk, and C. F. Quate, J. Chem. Phys. **86**, 6034 (1987).
[4] J. K. Gimszewski, E. Stoll, and R. R. Schlittler, Surf. Sci. **181**, 267 (1986).
[5] G. Binnig, Bull. Am. Phys. Soc. **31**, 217 (1986).
[6] J. S. Foster, J. E. Frommer, and P. C. Arnett, Nature **331**, 324 (1988).
[7] J. S. Foster and J. E. Frommer (unpublished).
[8] O. Marti, H. O. Ribi, B. Drake, T. R. Albrecht, C. F. Quate, and P. K. Hansma, Science **239**, 50 (1988).
[9] G. G. Roberts, P. S. Vincent, and W. A. Barlow, Phys. Technol. **12**, 69 (1981).
[10] A. Cemel, T. Fort, and J. B. Lando, J. Polym. Sci. Pt. A1 **10**, 2061 (1972).
[11] R. H. Tredgold and C. S. Winter, J. Phys. D **15**, L55-58 (1982).
[12] M. A. McCord and R. F. W. Pease, Appl. Phys. Lett. **50**, 9 (1987).
[13] N. A. Plate, V. P. Shibaev, B. S. Petrukhin, Y. A. Zubov, and V. A. Kargin, J. Poly. Sci. **9**, 2291 (1971).
[14] R. M. Silver, E. E. Ehrichs, and A. L. DeLozanne, Appl. Phys. Lett. **51**, 247 (1987).
[15] J. Schneir, P. K. Hansma, V. Elings, J. Gurley, K. Wickramasinghe, and R. Sonnenfeld (to be published).
[16] Secondary standard, purchased from Scientific Polymer Products, Inc., Ontario, NY.
[17] Langmuir Trough IV, Joyce-Loebl, London, England.
[18] G. Binnig, H. Fuchs, Ch. Gerber, H. Rohrer, E. Stoll, and E. Tosatti, Europhys. Lett. **1**, 31 (1986).
[19] S. A. Greenberg and T. Alfrey, J. Am. Chem. Soc. **76**, 6280 (1954).
[20] H. W. S. Hsieh, B. Post, and H. Morawetz, J. Polym. Sci. **14**, 1241 (1976).
[21] S. J. Mumby, J. D. Swalen, and J. F. Rabolt, Macromolecules **19**, 1054 (1986),
[22] A. Bryant, D. P. E. Smith, and C. F. Quate, Appl. Phys. Lett. **48**, 832 (1986).
[23] G. Binnig and D. P. E. Smith, Rev. Sci. Instrum. **57**, 1688 (1986).
[24] T. R. Albrecht and C. F. Quate, J. Appl. Phys. **62**, 2599 (1987).
[25] G. Binnig, Ch. Gerber, E. Stoll, T. R. Albrecht, and C. F. Quate, Europhys. Lett. **3**, 1281 (1987).
[26] Arlunya TF 5111, The Dindima Group Pty. Ltd., Melbourne, Victoria, Australia.
[27] H. J. Mamin, E. Ganz, D. W. Abraham, R. E. Thomson, and J. Clarke, Phys. Rev. B **34**, 9015 (1986).
[28] S. Park, J. Nogami, and C. F. Quate, Phys. Rev. B **36**, 2863 (1987).
[29] H. A. Mizes, S. Park, and W. A. Harrison, Phys. Rev. B **36**, 4491 (1987).
[30] See, P. H. Geil, *Polymer Single Crystals* (Interscience, New York, 1963).
[31] T. R. Albrecht, H. A. Mizes, J. Nogami, S. Park, and C. F. Quate, Appl. Phys. Lett. **10**, 362 (1988).
[32] T. R. Albrecht and C. F. Quate, J. Vac. Sci. Technol. A **6**, 271 (1988).
[33] H. A. Mizes and J. S. Foster (unpublished).
[34] I. Haller, M. Hatzakis, and R. Srinivasan, IBM J. Res. Dev. **12**, 251 (1968).
[35] M. A. McCord, Ph.D. thesis (Dept. of Electrical Engineering, Stanford University, 1987).
[36] M. M. Dovek, T. R. Albrecht, W. J. Kuan, C. A. Lang, R. Emch, P. Grütter, C. W. Frank, R. F. W. Pease, and C. F. Quate (unpublished).